

Original Research

Effect of SKF96365 on Myocardial Fibrosis in Type-II Diabetic Rats

Huan-zhi Liu¹, Wei Wu^{1,*}¹Department of Emergency, The First Affiliated Hospital of China Medical University, 110001 Shenyang, Liaoning, China*Correspondence: wei1740wei@126.com (Wei Wu)

Academic Editor: Natascia Tiso

Submitted: 25 August 2022 Revised: 16 February 2023 Accepted: 22 February 2023 Published: 27 September 2023

Abstract

Background: Diabetes mellitus type 2 is a risk factor for developing heart failure and myocardial fibrosis, but there is no specific therapy for diabetic heart disease. 1-[2-(4-methoxyphenyl)]-2-[3-(4-methoxyphenyl) propoxy]ethyl-1H-imidazole (SKF96365) is regarded as an inhibitor of receptor-mediated calcium ion (Ca^{2+}) entry. This study aimed to explore the effects of SKF96365 on diabetic myocardial fibrosis. **Methods:** A type 2 diabetic rat model induced by a high-sugar and high-fat diet combined with streptozotocin was established. Thirty specific pathogen-free male Wistar rats were divided randomly into three groups: group A (the blank control group), group B (the diabetes group) and group C (the diabetes + transient receptor potential canonical channel [TRPC] blocker intervention group). Group C was given 0.74- $\mu\text{mol}/\text{kg}$ SKF96365 by intraperitoneal injection, and groups A and B were given the same amount of normal saline by intraperitoneal injection. The weight and blood sugar of the rats were monitored. After 12 weeks, the weight of the whole heart and the left ventricle was measured, and the heart and the left ventricular weight ratios were calculated. Haematoxylin–eosin (HE) staining was used to observe pathological changes in the myocardial tissue and the distribution of nuclei. Masson staining was used to identify collagen and muscle fibres, and the myocardial collagen volume fraction (CVF) was calculated. Semi-quantitative reverse transcription–polymerase chain reaction was used to detect the messenger ribonucleic acid (mRNA) expression of SKF96365 target genes. A value of $p < 0.05$ indicated that the difference between the groups was statistically significant. **Results:** Compared with the weight of the rats in group A, the weight of those in groups B and C decreased, while blood sugar, whole heart weight and left ventricular weight increased ($p < 0.05$). There was no significant difference in body weight between the rats in groups B and C ($p > 0.05$). The HE staining results showed that the arrangement of cardiomyocytes in groups B and C was irregular, and focal necrosis was seen in severe cases. The degree of diabetic cardiomyopathy (DCM) in group C was less severe than that in group B. Masson staining showed that the CVF increased in groups B and C, with group B $>$ group C ($p < 0.05$); the mRNA expressions of TRPC3 and TRPC6 were upregulated in groups A, B and C, and the mRNA expressions of TRPC3 and TRPC6 in group C were downregulated compared with those in group B ($p < 0.05$). Compared with the expression levels of SKF96365 target genes (*STIM1*, *Orai1* and *Homer1*) in group A, those in group B were lower, while the administration of SKF96365 in group C did not affect the expression levels of those genes. **Conclusions:** SKF96365 can effectively improve myocardial fibrosis in type-II diabetic rats.

Keywords: diabetes; myocardial fibrosis; SKF96365; SOCE; TRPC

1. Introduction

Diabetes mellitus (DM) is a general term for a group of metabolic diseases characterised mainly by hyperglycaemia and caused by abnormal insulin secretion or action defects. DM has now become one of the major diseases that threaten human longevity. According to International Diabetes Federation statistics, the number of deaths due to diabetes and its related complications is more than 4.6 million globally each year, and the annual medical expenditure for patients with diabetes is more than 450 billion US dollars [1]. Diabetic cardiomyopathy (DCM) is one of the most serious complications of DM, with high mortality and morbidity [2,3]. Most patients with DCM are in the subclinical stage, during which the main pathological changes are cardiomyocyte hypertrophy and myocardial fibrosis, and gradually develop abnormal cardiac systolic function with the progression of the disease [4]. The pathogenesis of DCM is complex, and its specific mechanism is not yet fully understood.

Calcium ion (Ca^{2+}) is an essential second messenger that induces a signalling cascade in many immune responses, and Ca^{2+} influx is mediated by Ca^{2+} channels distributed in various cells. Transient receptor potential canonical channel (TRPC) and store-operated calcium entry (SOCE) mediated by stromal interaction molecule1 (STIM1) and ORAI calcium release-activated calcium modulator 1 (Orai1) play pivotal roles in mediating Ca^{2+} influx in a variety of cells. 1-[2-(4-methoxyphenyl)-2-[3-(4-methoxyphenyl) propoxy]ethyl-1H-imidazole (SKF96365) is a small-molecule compound acting as a non-selective inhibitor of TRPC, SOCE and voltage-gated Ca^{2+} channels that has been proven to suppress cellular Ca^{2+} influx via the inhibition of these Ca^{2+} channels. The TRPC subfamily includes seven members (TRPC1–7), which are non-selective, calcium ion- (Ca^{2+}) permeable cation channels that participate in a series of physiological events mediated by Ca^{2+} signal transduction pathways [5]. Studies have shown that Ca^{2+} can enter cardiomyocytes



through Transient Receptor Potential (TRP) channels [6]. Reports show that transient receptor potential cation channel, subfamily M, member 7 (TRPM7) is essential in transforming growth factor- β 1-mediated fibrogenesis, and TRPC3 has been demonstrated to play an essential role in regulating fibroblast function. Thus, Ca^{2+} -permeable TRP channels may serve as potential novel targets for developing anti-fibrotic drugs [7]. Hu *et al.* [8] also found that the TRPC1 protein is abundantly expressed in cardiomyocytes and is closely related to cardiac hypertrophy, which can act as a regulator of Ca^{2+} concentration and contractility of mammalian cardiomyocytes. Kuwahara *et al.* [9] showed that TRPC6 fulfils a calcineurin signalling circuit during pathologic cardiac remodelling. These studies suggest the important role of TRPC family members in myocardial function.

SKF96365 has been widely used to study the function of TRPC channels [10–14]. Originally identified as a blocker of receptor-mediated calcium entry, SKF96365 is widely used diagnostically as a blocker of TRPC channels. It has been reported that SKF96365 can inhibit AngII-induced cardiomyocyte hypertrophy [10], but its therapeutic effect and mechanism in DCM are unclear. In this study, a rat model of type-II diabetes was established and SKF96365 was administered. The relevant indicators and pathological changes in myocardial fibrosis were observed and compared to explore the effect of SKF96365 on diabetic myocardial fibrosis. The findings will provide a theoretical basis for the early intervention of patients with diabetes to improve the degree of DCM and provide new ideas for the prevention and treatment of cardiomyopathy in patients with diabetes.

2. Materials and Methods

2.1 Experimental Animals

Thirty healthy four-week-old specific pathogen-free (SPF) Wistar male rats (purchased from Beijing Weitong Lihua Laboratory Animal Technology Co., Ltd., SYXX [JING] 2022-0052, China), weighing 180–200 g, were selected for the experiment. The rats were housed at a constant temperature (21 °C–23 °C) and humidity (45%–65%) in a rearing room that maintained a 12-hour light–dark cycle, with free access to food and water. All animal experiments were performed according to the Helsinki Declaration, and this experimental protocol was approved by the Experimental Animal Ethics Committee (approval number: CMU2013070).

2.2 Reagents and Instruments

The main reagents included the following: streptozotocin (STZ) (Sigma, St. Louis, Missouri, USA), TRIzol reagent (Ambion, Carlsbad, California, USA), SKF96365 (ABCAM, UK), Murine leukaemia virus (MuLV) reverse transcriptase kit (Applied Biosystems, Foster City, CA, USA), Tris (Invitrogen, Carlsbad, USA), ethylene diamine

tetra acetic acid (Invitrogen), Agarose (Invitrogen), Paraffin (Leica, Solms, Germany), Radioimmunoprecipitation (RIPA) lysis buffer (Applygen Technologies Inc, Beijing, China), protease inhibitor (Sigma), phosphatase inhibitor (Sigma), chemiluminescence Western Blot Detection Reagent kit (GE Healthcare, Parramatta, Australia) and a Takara reverse transcription–polymerase chain reaction (RT-PCR) Kit (Bao Bioengineering Dalian Co., Ltd., Dalian, China).

The main instruments were as follows: an analytical balance (Sartorius, Gottingen, Germany), a blood glucose meter (Jiangsu Yuyue Medical Equipment Co., Ltd., Danyang, China), a pH meter (Thermo Scientific, Massachusetts, USA), a 4 °C low-temperature refrigerator (Electrolux, Stockholm, Sweden), an incubator (Shanghai Boxun Industrial Co., Ltd. Shanghai, China), a paraffin embedding machine (Leica, Solms, Germany), a paraffin microtome (Leica, Germany), an optical microscope (Olympus, Tokyo, Japan), a low-temperature high-speed centrifuge (Eppendorf, Hamburg, Germany), an ultraviolet spectrophotometer (Shimadzu, Kyoto, Japan), a micropipette (Eppendorf, Hamburg, Germany), a PCR amplifier (Biometra, Jena, Germany), Odyssey image scanning software v3.0 (LiCOR Biosciences, Lincoln, NE, USA), polyvinylidene difluoride (PVDF) membranes (Millipore, Bedford, MA, USA) and an electrophoresis device (Beijing Liuyi Instrument Factory, Beijing, China).

2.3 Preparation of Rat Type-II Diabetes Model

The preparation of the rat model of type-II diabetes was performed in accordance with the method of Reed *et al.* [15]. Four-week-old SPF male Wistar rats were given a high-sugar and high-fat diet (60% fat, 22% carbohydrate [sucrose] and 18% protein). After 1 week of acclimatisation to the environment, total calories of about 5.5 kcal/g were given for 8 weeks. After 24 hours of fasting, an intraperitoneal injection of 1% STZ 35 at mg/kg was administered, and the indicators were measured after 24 and 48 h. The following were considered to indicate a successful model: fasting blood glucose >11.1 mmol/L, postprandial blood glucose >16.7 mmol/L, glycated haemoglobin >6%, urine sugar qualitative above +++ and the presence of polydipsia and polyphagia. The control group was injected with the same volume of sodium citrate/citric acid buffer as that of STZ injected into the model group. If the modelling failed, the following procedure took place: After 72 hours of the first intraperitoneal injection, the rats that failed to model were given another intraperitoneal injection of STZ (17.5 mg/kg). 24 h after the second intraperitoneal injection, the various indicators were re-examined using the modeling criteria described above.

2.4 Experiment Grouping and Processing

Thirty healthy male Wistar rats were randomly divided into three groups: group A (the blank control group),

group B (the diabetes control group) and group C (the diabetes + SKF96365 intervention group), each containing 10 rats. The rats in group B and group C were modelled normally, and the rats in group C were given a 0.74- μ mol/kg SKF96365 intraperitoneal injection after successful modelling, once a day for 12 weeks. During this period, the rats in group A were given a normal diet, while those in groups B and C continued to eat a high-sugar and high-fat diet, and their body weight and blood sugar were monitored daily.

After 12 weeks, the rats were injected with 3% pentobarbital sodium (40 mg/kg) intraperitoneally to euthanize them. The weight of the whole of the heart was recorded, and the left ventricle was isolated and weighed on its own. The heart-to-body (whole heart weight/body weight) and left-ventricle-to-body (left ventricular weight/body weight) ratios were calculated.

2.5 Tibia Length Measurement

The tibia was removed, as was the surrounding soft tissue, and the length of the tibia was measured using a vernier calliper (accuracy 0.02 mm), with the main ruler parallel to the tibia length and the two ends of the tibia fully clamped. The shortest distance measured was recorded.

2.6 Haematoxylin and Eosin Staining

Haematoxylin and eosin (HE) staining was performed in accordance with the method of Yang *et al.* [16]. Cardiac tissue was fixed in 4% paraformaldehyde for 24 h and then dehydrated and embedded in paraffin. The paraffin block was cut into 4- μ m-thick sections using a rotary microtome. The sections were dewaxed with xylene, dehydrated with different concentrations of ethanol, nuclear stained with haematoxylin and differentiated using a differentiation medium. Then, they underwent eosin cytoplasmic staining, were dehydrated with different concentrations of ethanol, cleaned with xylene and sealed with neutral resin; subsequently, a microscopic examination was performed, and the resulting images were analysed.

2.7 Masson Staining

Masson staining was performed with reference to Li C *et al.* [17]. Cardiac tissue was fixed in 4% paraformaldehyde for 48 h at 4 °C, dehydrated and embedded in paraffin. The paraffin block was cut into 4- μ m-thick sections using a rotary microtome. Staining was performed using Masson's trichrome, followed by imaging under a microscope (Olympus™, Japan). ImageJ software (V1.8.0, National Institutes of Health, Bethesda, MD, USA) was used to quantify areas of fibrosis and reflect the percentage of blue positive-stained areas in the total tissue area to calculate the myocardial collagen volume fraction (CVF).

2.8 Ribonucleic Acid Extraction and Semi-Quantitative Reverse Transcription–Polymerase Chain Reaction Analysis

Total ribonucleic acid (RNA) extraction from myocardial tissue was performed using the reagent TRIzol, and complementary deoxyribonucleic acid was synthesised using the MuLV reverse transcriptase kit. Semi-quantitative reverse RT-PCR was performed using the polymerase in the Takara RT-PCR kit. After the PCR products were verified using gel electrophoresis, they were photographed and stored in a gel imaging system, and the grey values were calculated. Densitometric analysis was performed to quantify the messenger RNA (mRNA) levels of SKF96365 target genes relative to the expression of the endogenous reference gene β -actin. The primer sequences are shown in Table 1.

Table 1. Primer sequences for semi quantitative reverse transcription–polymerase chain reaction (qRT-PCR).

Gene name	Explain	Primer sequence
<i>TRPC3</i>	Forward	5'-GGCTATGTTCTTTATGGGATAT-3'
	Reverse	5'-CCATCATCAAAGTAGGAGAGCC-3'
<i>TRPC6</i>	Forward	5'-ATCGGCTACGTTCTGTATGGTGCT-3'
	Reverse	5'-GGAAAACCACAATTTGGCCCTTGC-3'
<i>STIM1</i>	Forward	5'-CGCTGAACCATGGCCTAGAT-3'
	Reverse	5'-GGGAATTCGTGTGTTTCGGC-3'
<i>Orai1</i>	Forward	5'-GAACAACAGCAATCCGGAGC-3'
	Reverse	5'-CACCTCGGAGTAACTCTGGC-3'
<i>Homer1</i>	Forward	5'-CACGCTCAAGGGGAACAATG-3'
	Reverse	5'-AACACATTCCAGCTCCGTGA-3'
β -actin	Forward	5'-TCAGGTCATCACTATCGGCAAT-3'
	Reverse	5'-AAAGAAAGGGTGTAAAACGCA-3'

2.9 Western Blot

Tissues were lysed by adding RIPA lysis buffer containing protease inhibitor and phosphatase inhibitor in concentrations specified by the respective manufacturers. The lysate was centrifuged at 12,000 g for 10 min, and the supernatant was collected. Protein concentration was determined using a bicinchoninic acid assay. Then, the samples were subjected to sodium dodecyl sulphate–polyacrylamide gel electrophoresis, and the proteins were then transferred onto PVDF membranes. The PVDF membranes were blocked with 5% skimmed milk dissolved in Tris-buffered saline containing 0.1% Tween 20 (TBS-T); then, they were incubated overnight at 4 °C with specific antibodies against *STIM1*, *Orai1*, *Homer1* and glyceraldehyde 3-phosphate dehydrogenase (Cambridge, MA, USA). The membranes were washed in TBS-T and incubated with the appropriate horseradish peroxidase-conjugated secondary antibody for 1 h at 25 °C. Finally, the membranes were washed with TBS-T and developed using an enhanced chemilumines-

cence Western blot detection reagent kit. Odyssey image scanning software v3.0 (Lincoln, Nebraska, USA) was used to obtain images of the membranes.

2.10 Statistical Analysis

Statistical analysis was performed using SPSS 19.0 software (IBM Corp., Chicago, IL, USA). All data are presented as mean \pm standard deviation. A one-way analysis of variance was used to analyse the experimental data of the groups. First, a homogeneity test of variance was performed. If the variance showed homogeneity, the least-significant difference method was used. When the variance was not homogeneous, a rank-sum test or Pearson's correlation analysis was used. A value of $p < 0.05$ indicated a statistically significant difference between groups.

3. Results

3.1 Comparison of Routine Indicators

The body weight and postprandial blood glucose indexes of the rats in all three groups were detected, and the results are shown in Fig. 1. Compared with the weight of the rats in group A, the weights in groups B and C decreased, and the difference was statistically significant ($p < 0.05$). There was no significant difference in body weight between the rats in group B and group C ($p > 0.05$) (Fig. 1A). The postprandial blood glucose levels of the rats in groups B and C were significantly higher than those of the rats in group A ($p < 0.05$). Compared with the postprandial blood glucose of the rats in group B, that of the rats in group C, who were given SKF96365, decreased, and the difference was statistically significant ($p < 0.05$) (Fig. 1B).

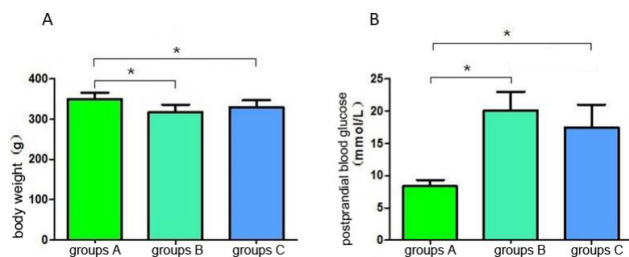


Fig. 1. SKF96365 promote postprandial glucose decline. (A) Comparison of body weight of rats in each group. (B) The postprandial blood glucose of rats in each group. * $p < 0.05$.

3.2 Comparison of Rat Cardiac Indexes

Compared with the whole heart weight of the rats in group A, that of the rats in group B increased; the difference was statistically significant ($p < 0.05$), but there was no significant difference between the weights in group C and groups A and B ($p > 0.05$) (Fig. 2A). Compared with the weight of the left ventricle in group A, the weight of the left ventricle in groups B and C increased, showing a statistical significance ($p < 0.05$), although there was no significant difference between the ventricular weights in groups B and

C ($p > 0.05$) (Fig. 2B). Compared with the ratios in group A, the heart (Fig. 2C) and left ventricular ratios (Fig. 2D) of the rats in group B were significantly increased, and the difference between the ratios in group C and groups A and B was statistically significant ($p < 0.05$). In addition, the ratio of heart weight to tibial length was used to assess myocardial hypertrophy. The results showed that the severity of myocardial hypertrophy was greater in group B than in group A and was inhibited after the application of the blockers ($p < 0.05$) (Fig. 2E).

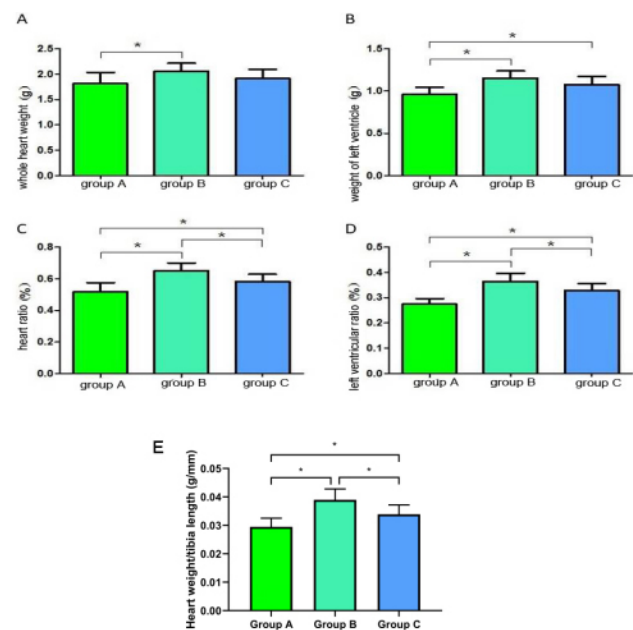


Fig. 2. Comparison of cardiac physiological indexes of rats in each group. (A) Whole heart weight comparison. (B) Left ventricular weight comparison. (C) Heart weight ratio. (D) Left ventricular weight ratio. (E) The ratio of heart weight to tibial length was used to assess myocardial hypertrophy. * $p < 0.05$.

3.3 Haematoxylin and Eosin Staining

Haematoxylin and eosin staining was used to observe the pathological changes in the rats' myocardia. The HE staining results showed that the myocardia of the rats in group A were arranged regularly and neatly; the intercellular space was small, and the myocardial texture was visible.

Compared with the rat cardiomyocytes in group A, those in group B were hypertrophied, the arrangement of cardiomyocytes was disordered, the myocardial texture was blurred (Fig. 3A), the intercellular space was enlarged, and the average width of the cardiomyocytes was increased (Fig. 3B). The degree of myocardial cell hypertrophy in group C was lower than that in group B. Compared with the myocardial arrangement in group B, the myocardial arrangement was better in group C, and the texture of myocardial fibres was slightly blurred. The average width of the cardiomyocytes in group C was significantly lower than that in group B (Fig. 3).

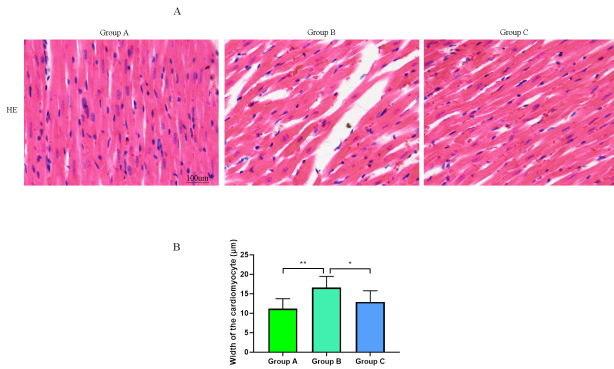


Fig. 3. Haematoxylin–eosin (HE) staining of rat heart tissue in each group (200×). (A) Images of HE staining. (B) Quantification of cardiomyocyte width in HE stained images. * $p < 0.05$, ** $p < 0.01$.

3.4 Masson Staining

Masson staining was performed on rat myocardial tissues to observe the degree of fibrosis. The staining results showed that myocardial fibres were red, and myocardial collagen fibres were blue–purple. The collagen fibres in group A were evenly distributed; compared with the collagen fibres in group A, those in group B were increased and their distribution was uneven, whereas the collagen fibres in group C were reduced compared with those in group B (Fig. 4A). The myocardial CVF of the groups showed that group B > group C > group A, and the difference between the groups was statistically significant ($p < 0.05$) (Fig. 4B).

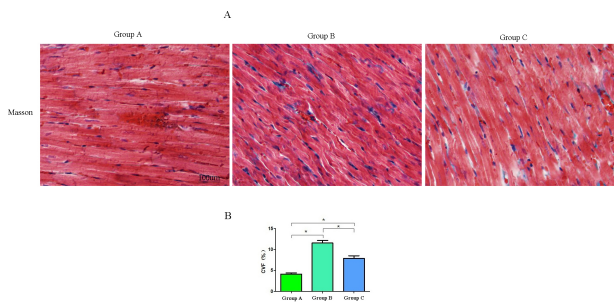


Fig. 4. Masson staining. (A) Images of rat heart tissue in each group (200×). (B) The comparison of myocardial collagen volume fraction. * $p < 0.05$.

3.5 The Relative Expression Levels of SKF96365 Target Genes and Target Proteins

The semi-quantitative results showed that the myocardial TRPC3 mRNA and TRPC6 mRNA expressions in groups B and C were significantly higher than those in group A ($p < 0.05$). The expression levels of TRPC3 mRNA and TRPC6 mRNA in group C were downregulated

compared with those in group B, and the difference was statistically significant ($p < 0.05$) (Fig. 5). SKF96365 has been shown to be an antagonist of the physiological process of SOCE. Therefore, the expression levels of other targets of SKF96365 in the physiological process of SOCE, such as *STIM1*, *Orai1* and *Homer1*, were examined, and the results are shown in Fig. 6. Compared with the levels in group A, the mRNA and protein levels of all three genes (*STIM1*, *Orai1* and *Homer1*) were lower in group B, while the administration of blocker SKF96365 in group C did not affect their expression levels.

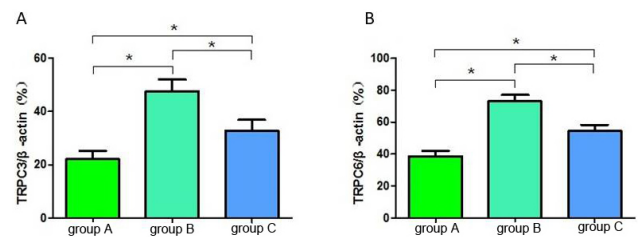


Fig. 5. The relative gray value ratio of TRPC3 (A) and TRPC6 (B) in each group of rats. * $p < 0.05$.

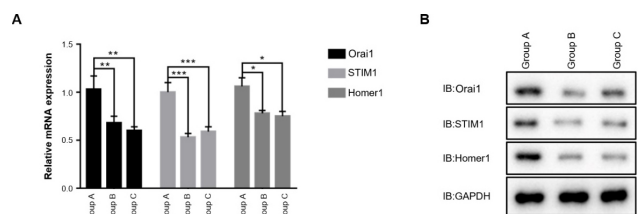


Fig. 6. The mRNA (A) and protein (B) expression of other targets of SKF96365 in each group of rats. * $p < 0.05$, ** $p < 0.01$, *** $p < 0.001$.

4. Discussion

Cardiomyocyte fibrosis is the main obvious pathological feature of DCM, which increases myocardial stiffness, causing diastolic dysfunction [18]. Luo *et al.*'s [19] study of diabetic rats showed eccentric myocardial hypertrophy, and they found that the ratio of heart to body weight was extremely large, the ultrastructure of the left ventricle was severely damaged, and the myocardial interstitial fibrosis was aggravated. The present study showed that the heart-to-body-weight ratio and the left-ventricle-to-body-weight ratio of the diabetic model rats were significantly higher than those of the normal rats, which suggested that the diabetic rats had developed cardiac lesions. Further pathological HE staining showed myocardial hypertrophy, disordered myocardial cells, enlarged intercellular spaces and blurred myocardial texture. In addition, Masson staining revealed severe myocardial fibrosis in the diabetic rats' myocardia.

Short-term hyperinsulinemia in DM may regulate glucose uptake through Phosphoinositide-3 kinase (PI3K)/protein kinase B or AKT serine/threonine kinase (Akt), thereby stimulating cell growth and causing cardiac hypertrophy [20]. Hyperglycaemia activates signalling molecules (such as c-Jun N-terminal kinase 1) in cardiomyocytes, and oxidative stress also mediates both cardiomyocyte hypertrophy and fibrosis [21,22]. In addition, abnormal vascular growth factors and changes in tiny blood vessels, especially arteries and capillaries, are prone to phenomena such as fatty infiltration, intimal and subintimal hyperplasia and basement membrane thickening. It further blocks the discharge of harmful substances and aggravates myocardial damage [23]. The complexity of the pathogenesis of DCM implies that more time and energy should be invested in its understanding.

Transient receptor potential canonical channels are a group of ion channels with many physiological functions [24]. After the expression products of the *TRPC* gene combine with each other to form homo- or hetero-polymers *in vivo*, they can form non-selective ion channels through which Ca^{2+} , sodium ions and magnesium ions can enter cells. The TRPC family has seven subtype members. TRPC3 is distributed mainly in brain tissue, smooth muscle cells and vascular endothelial cells; TRPC6 is widely expressed throughout the vasculature and is detectable in the lung and muscle, and limited amounts of TRPC7 are expressed in the eye, heart and lung [25]. As they are distributed in different tissues and organs, these TRPCs play different roles after activation [26]. It is also known that TRPC is permeable to Ca^{2+} , which participates in various physiological and biochemical body reactions and regulates many physiological functions in the body. Studies have found that abnormal Ca^{2+} metabolism in cardiomyocytes and abnormal cardiac sarcoplasmic reticulum Ca^{2+} concentration can lead to decreased cardiac compliance and diastolic function [27], which strongly suggests the potential function of TRPC in cardiomyopathy.

In this study, compared with normal rats, diabetic rats showed morphological changes, including increased heart mass, myocardial hypertrophy and upregulated expression of *TRPC3* and *TRPC6* genes in heart tissue, suggesting that TRPC3 and TRPC6 may be involved in the physiological process of the development of DCM. During DCM development, TRPC3/Nox2-induced oxidative stress processes have been shown to be involved in cardiac fibrosis [28]. However, studies by Oda *et al.* [29] showed that the deletion of TRPC6 exacerbated heart failure in diabetic mice and oxidative stress, while the deletion of TRPC6 had no significant effect on myocardial fibrosis in DCM mice. Although TRPC3 and TRPC6 have a high degree of functional similarity, TRPC3 and TRPC6 differ substantially in their basal channel activities. Oda S *et al.* [29] reported that TRPC6 counteracts the TRPC3–Nox2 protein complex, leading to the attenuation of hyperglycaemia-induced

heart failure in mice, which may not be related to TRPC6 channel activity. The specific function of TRPC6 in DCM still needs further exploration.

The protective effects of SKF96365 on the nervous system, renal system and vascular system in diabetic animal models have been preliminarily confirmed [28,30]. In the present study, the administration of SKF96365 to type-II diabetes model rats significantly improved the degree of diabetic myocardial fibrosis. In the process of ventricular remodelling in DCM, the intracellular calcium signal transduction pathway plays an important role in mediating myocardial hypertrophy and myocardial fibrosis. In the intracellular Ca^{2+} signalling pathway, extracellular stimuli, such as angiotensin II, vascular endothelin-1 and norepinephrine, can activate the Gq protein-coupled receptor pathway and/or the tyrosine kinase pathway to activate phospholipase C, thereby inducing the release of Ca^{2+} . The increase of Ca^{2+} concentration induces the activation of calcineurin, which further leads to the dephosphorylation of the nuclear factor of activated T cells, exposes its nuclear localisation signal and then translocates it into the nucleus. The interaction of multiple transcription factors in the nucleus, including GATA binding protein 4 (GATA4), activates a variety of genes related to myocardial hypertrophy and increases the synthesis of nucleic acids and proteins in cardiomyocytes, thereby increasing the volume of cardiomyocytes and causing the occurrence of pathological changes, such as myocardial hypertrophy and myocardial fibrosis [9,31,32]. In addition, high glucose exposure increases TRPC expression and Ca^{2+} entry in monocytes [33]. Monocyte activation in the heart can trigger and promote fibrosis. SKF96365 may block the flow of Ca^{2+} , thereby regulating its signalling pathway and ultimately, inhibiting cardiomyopathy; furthermore, it may reduce cardiac hypertrophy by inhibiting TRPC-induced oxidative stress [12], the specific mechanism of which needs further exploration.

There are certain limitations to this study. First, due to the constraints of available resources and the timeframe of the research project, the study used a relatively primitive type-II diabetic rat model, wherein the rats were treated with a high-sugar and high-fat diet in combination with a low-dose STZ injection to induce insulin-resistance symptoms. However, although this method is relatively stable, reliable and easy to implement, it lacks a unified standard, and there is no consensus on the modelling standard of type-II diabetic rats. According to published studies [34], this diabetic rat model is lighter in weight and has a significant increase in heart and liver coefficients compared with normal rats. Therefore, in this study, the rats in the model-prepared groups (groups B and C) lost weight. Although there are related experimental studies that used this method to simulate type-II diabetic rats, this modelling method is not used in most higher-level experiments, and spontaneous diabetes models, such as ob/ob mice (Leptin Deficiency Mouse Model), db/db mice (derived from autosomal recessive

sive inheritance of C57BL/KsJ inbred strain, belong to the type 2 diabetes model), obese Zucker rats, Wistar–Kyoto rats and SHR/N-cp rats, are more commonly used. The pathophysiological changes in these models are closer to those of clinical patients with type-II diabetes, so the results may have greater validation. Second, SKF96365 is not a specific TRPC inhibitor but more widely a SOCE inhibitor that acts against TRPC but also other actors, such as voltage-gated calcium channels [35]. There are significant overlapping physiological and pathophysiological associations between TRPC channels and low-pressure activated T-type calcium channels. In future studies, the authors will use gene editing to construct TRPC-deficient rats and specifically block *TRPC3/6* to further study the beneficial effect of TRPC on diabetic myocardial fibrosis.

5. Conclusions

This study found that in diabetic rats, the myocardial tissue was damaged, and the degree of myocardial fibrosis was high. SKF96365 significantly reduced both myocardial CVF and the cardiac and left ventricular ratios and significantly improved myocardial fibrosis in diabetic rats.

Abbreviations

TRPC, transient receptor potential channel; TRP, transient receptor potential; IDF, International Diabetes Federation; DM, diabetes mellitus; DCM, diabetes cardiomyopathy; STZ, streptozocin; UV, Ultraviolet; EDTA, Ethylene Diamine Tetraacetic Acid; HE, hematoxylin-eosin; PBS, phosphate buffered saline; CVF, collagen volume fraction; RT-PCR, reverse transcription-polymerase chain reaction; OD, optical density; Tris, Tris (Hydroxymethyl) aminomethane; EDTA, ethylene diamine tetraacetic acid; EB, ethidium bromide; PI3K, phosphatidylinositol 3-kinase; PKB, protein kinase B; JNK1, c-Jun N-terminal kinases-1; NFATs, nuclear factor of activated T cells; ANF, atrial natriuretic factor; BNP, brain natriuretic peptide; NFATs, nuclear factor of activated T cells.

Consent for Publication

Not applicable.

Availability of Data and Materials

The data that support the findings of this study are available from the corresponding author upon reasonable request.

Author Contributions

HL and WW conceived of the study, and participated in its design and coordination and helped to draft the manuscript. Both authors contributed to editorial changes in the manuscript. Both authors read and approved the final manuscript. Both authors have participated sufficiently in the work and agreed to be accountable for all aspects of the work).

Ethics Approval and Consent to Participate

This study was conducted in accordance with the Declaration of Helsinki and approved by the Ethics Committee of the First Affiliated Hospital of China Medical University (CMU2013070).

Acknowledgment

We would like to express our gratitude to all those who helped us during the writing of this manuscript.

Funding

This research received no external funding.

Conflict of Interest

The authors declare no conflict of interest.

References

- [1] Yao X, Pei X, Yang Y, Zhang H, Xia M, Huang R, *et al.* Distribution of diabetic retinopathy in diabetes mellitus patients and its association rules with other eye diseases. *Scientific Reports*. 2021; 11: 16993.
- [2] Wang J, Wang R, Li J, Yao Z. Rutin alleviates cardiomyocyte injury induced by high glucose through inhibiting apoptosis and endoplasmic reticulum stress. *Experimental and Therapeutic Medicine*. 2021; 22: 944.
- [3] Zhu HZ, Zhang LY, Zhai ME, Xia L, Cao Y, Xu L, *et al.* GDF11 Alleviates Pathological Myocardial Remodeling in Diabetic Cardiomyopathy Through SIRT1-Dependent Regulation of Oxidative Stress and Apoptosis. *Frontiers in Cell and Developmental Biology*. 2021; 9: 686848.
- [4] Yu Y, Zheng G. Troxerutin protects against diabetic cardiomyopathy through NF- κ B/AKT/IRS1 in a rat model of type 2 diabetes. *Molecular Medicine Reports*. 2017; 15: 3473–3478.
- [5] Wang B, Xiong S, Lin S, Xia W, Li Q, Zhao Z, *et al.* Enhanced Mitochondrial Transient Receptor Potential Channel, Canonical Type 3-Mediated Calcium Handling in the Vasculature From Hypertensive Rats. *Journal of the American Heart Association*. 2017; 6: e005812.
- [6] Gao H, Wang F, Wang W, Makarewich CA, Zhang H, Kubo H, *et al.* Ca(2+) influx through L-type Ca(2+) channels and transient receptor potential channels activates pathological hypertrophy signaling. *Journal of Molecular and Cellular Cardiology*. 2012; 53: 657–667.
- [7] Yue Z, Zhang Y, Xie J, Jiang J, Yue L. Transient receptor potential (TRP) channels and cardiac fibrosis. *Current Topics in Medicinal Chemistry*. 2013; 13: 270–282.
- [8] Hu Q, Ahmad AA, Seidel T, Hunter C, Streiff M, Nikolova L, *et al.* Location and function of transient receptor potential canonical channel 1 in ventricular myocytes. *Journal of Molecular and Cellular Cardiology*. 2020; 139: 113–123.
- [9] Kuwahara K, Wang Y, McAnally J, Richardson JA, Bassel-Duby R, Hill JA, *et al.* TRPC6 fulfills a calcineurin signaling circuit during pathologic cardiac remodeling. *Journal of Clinical Investigation*. 2006; 116: 3114–3126.
- [10] Cheng H, Li J, Wu Q, Zheng X, Gao Y, Yang Q, *et al.* Effect of SKF 96365 on cardiomyocyte hypertrophy induced by angiotensin II. *Molecular Medicine Reports*. 2020; 21: 806–814.
- [11] Krolik A, Diamandakis D, Zych A, Stafiej A, Salinska E. The involvement of TRP channels in memory formation and task retrieval in a passive avoidance task in one-day old chicks. *Neurobiology of Learning and Memory*. 2020; 171: 107209.
- [12] Lopez JR, Uryash A, Faury G, Estève E, Adams JA. Contribu-

- tion of TRPC Channels to Intracellular Ca²⁺ + Dyshomeostasis in Smooth Muscle From mdx Mice. *Frontiers in Physiology*. 2020; 11: 126.
- [13] Liu Z, Du Z, Li K, Han Y, Ren G, Yang Z. TRPC6-Mediated Ca²⁺ Entry Essential for the Regulation of Nano-ZnO Induced Autophagy in SH-SY5Y Cells. *Neurochemical Research*. 2020; 45: 1602–1613.
- [14] Jain PP, Hosokawa S, Xiong M, Babicheva A, Zhao T, Rodriguez M, *et al.* Revisiting the mechanism of hypoxic pulmonary vasoconstriction using isolated perfused / ventilated mouse lung. *Pulmonary Circulation*. 2020; 10: 2045894020956592.
- [15] Reed MJ, Meszaros K, Entes LJ, Claypool MD, Pinkett JG, Gadbois TM, *et al.* A new rat model of type 2 diabetes: the fat-fed, streptozotocin-treated rat. *Metabolism: Clinical and Experimental*. 2000; 49: 1390–1394.
- [16] Yang F, Qin Y, Wang Y, Meng S, Xian H, Che H, *et al.* Metformin Inhibits the NLRP3 Inflammasome via AMPK/mTOR-dependent Effects in Diabetic Cardiomyopathy. *International Journal of Biological Sciences*. 2019; 15: 1010–1019.
- [17] Li C, Zhang J, Xue M, Li X, Han F, Liu X, *et al.* SGLT2 inhibition with empagliflozin attenuates myocardial oxidative stress and fibrosis in diabetic mice heart. *Cardiovascular Diabetology*. 2019; 18: 1–13.
- [18] Meng K, Cai H, Cai S, Hong Y, Zhang X. Adiponectin Modified BMSCs Alleviate Heart Fibrosis via Inhibition TGF-beta1/Smad in Diabetic Rats. *Frontiers in Cell and Developmental Biology*. 2021; 9: 644160.
- [19] Luo B, Li B, Wang W, Liu X, Xia Y, Zhang C, *et al.* NLRP3 gene silencing ameliorates diabetic cardiomyopathy in a type 2 diabetes rat model. *PLoS ONE*. 2014; 9: e104771.
- [20] Ji R, Chou CL, Xu W, Chen XB, Woodward DF, Regan JW. EP1 prostanoid receptor coupling to G i/o up-regulates the expression of hypoxia-inducible factor-1 alpha through activation of a phosphoinositide-3 kinase signaling pathway. *Molecular Pharmacology*. 2010; 77: 1025–1036.
- [21] Bilim O, Takeishi Y, Kitahara T, Arimoto T, Niizeki T, Sasaki T, *et al.* Diacylglycerol kinase zeta inhibits myocardial atrophy and restores cardiac dysfunction in streptozotocin-induced diabetes mellitus. *Cardiovascular Diabetology*. 2008; 7: 2.
- [22] Zhang H, Chen X, Zong B, Yuan H, Wang Z, Wei Y, *et al.* Gypenosides improve diabetic cardiomyopathy by inhibiting ROS-mediated NLRP3 inflammasome activation. *Journal of Cellular and Molecular Medicine*. 2018; 22: 4437–4448.
- [23] Miyazawa M, Yasuda M, Fujita M, Hirabayashi K, Hirasawa T, Kajiwara H, *et al.* Granulosa cell tumor with activated mTOR-HIF-1alpha-VEGF pathway. *The Journal of Obstetrics and Gynaecology Research*. 2010; 36: 448–453.
- [24] Lin R, Bao X, Wang H, Zhu S, Liu Z, Chen Q, *et al.* TRPM2 promotes pancreatic cancer by PKC/MAPK pathway. *Cell Death & Disease*. 2021; 12: 585.
- [25] Lee K, Jo YY, Chung G, Jung JH, Kim YH, Park CK. Functional Importance of Transient Receptor Potential (TRP) Channels in Neurological Disorders. *Frontiers in Cell and Developmental Biology*. 2021; 9: 611773.
- [26] Amato A, Terzo S, Lentini L, Marchesa P, Mulè F. TRPM8 Channel Activation Reduces the Spontaneous Contractions in Human Distal Colon. *International Journal of Molecular Sciences*. 2020; 21: 5403.
- [27] Arvanitis DA, Vafiadaki E, Sanoudou D, Kranias EG. Histidine-rich calcium binding protein: the new regulator of sarcoplasmic reticulum calcium cycling. *Journal of Molecular and Cellular Cardiology*. 2011; 50: 43–49.
- [28] Tang SG, Liu XY, Wang SP, Wang HH, Jovanović A, Tan W. Trimetazidine prevents diabetic cardiomyopathy by inhibiting Nox2/TRPC3-induced oxidative stress. *Journal of Pharmacological Sciences*. 2019; 139: 311–318.
- [29] Oda S, Numaga-Tomita T, Kitajima N, Toyama T, Harada E, Shimauchi T, *et al.* TRPC6 counteracts TRPC3-Nox2 protein complex leading to attenuation of hyperglycemia-induced heart failure in mice. *Scientific Reports*. 2017; 7: 7511.
- [30] Liu D, Zhu Z, Tepel M. The role of transient receptor potential channels in metabolic syndrome. *Hypertension Research*. 2008; 31: 1989–1995.
- [31] Amasaki Y. Calcineurin inhibitors and calcineurin-NFAT system. *Nihon Rinsho Meneki Gakkai Kaishi*. 2010; 33: 249–261. (In Japanese)
- [32] Horiba M, Muto T, Ueda N, Ophhof T, Miwa K, Hojo M, *et al.* T-type Ca²⁺ channel blockers prevent cardiac cell hypertrophy through an inhibition of calcineurin-NFAT3 activation as well as L-type Ca²⁺ channel blockers. *Life Sciences*. 2008; 82: 554–560.
- [33] Wuensch T, Thilo F, Krueger K, Scholze A, Ristow M, Tepel M. High glucose-induced oxidative stress increases transient receptor potential channel expression in human monocytes. *Diabetes*. 2010; 59: 844–849.
- [34] Tian J, Zhang M, Suo M, Liu D, Wang X, Liu M, *et al.* Dapagliflozin alleviates cardiac fibrosis through suppressing EndMT and fibroblast activation via AMPK α /TGF- β /Smad signalling in type 2 diabetic rats. *Journal of Cellular and Molecular Medicine*. 2021; 25: 7642–7659.
- [35] Singh A, Hildebrand ME, Garcia E, Snutch TP. The transient receptor potential channel antagonist SKF96365 is a potent blocker of low-voltage-activated T-type calcium channels. *British Journal of Pharmacology*. 2010; 160: 1464–1475.